Received: 5 November 2024 | Revised: 19 March 2025 | Accepted: 20 March 2025

DOI: 10.1002/dad2.70110

Alzheimer's & Dementia
Diagnosis, Assessment & Disease Monitoring

RESEARCH ARTICLE

Cerebrospinal fluid YKL-40 relates to white matter hyperintensity progression in females but not males over a 6-year period

Amalia J. Peterson[1,2] | **Yunyi Sun**[3] | **Derek B. Archer**[1,2] | **Hailey A. Adegboye**[1] | **Elizabeth E. Moore**[1,4] | **Isabella Deberghes**[1] | **Kimberly R. Pechman**[1] | **Niranjana Shashikumar**[1] | **W. Hudson Robb**[1] | **Abigail W. Workmeister**[1] | **T. Bryan Jackson**[1] | **Dandan Liu**[1,3] | **Logan Dumitrescu**[1,2] | **L. Taylor Davis**[1,5] | **Bennett A. Landman**[1,2,5,6] | **Kaj Blennow**[7,8] | **Henrik Zetterberg**[7,8,9,10,11,12] | **Timothy J. Hohman**[1,2] | **Angela L. Jefferson**[1,2,13]

[1]Vanderbilt Memory and Alzheimer's Center, Vanderbilt University Medical Center, Nashville, Tennessee, USA

[2]Department of Neurology, Vanderbilt University Medical Center, Nashville, Tennessee, USA

[3]Department of Biostatistics, Vanderbilt University Medical Center, Nashville, Tennessee, USA

[4]Department of Neurology, Mass General Brigham, Boston, Massachusetts, USA

[5]Department of Radiology and Radiological Sciences, Vanderbilt University Medical Center, Nashville, Tennessee, USA

[6]Department of Electrical Engineering and Computer Science, Vanderbilt University, Nashville, Tennessee, USA

[7]Department of Psychiatry and Neurochemistry, Institute of Neuroscience and Physiology, The Sahlgrenska Academy at University of Gothenburg, Mölndal, Sweden

[8]Clinical Neurochemistry Lab, Sahlgrenska University Hospital, Mölndal, Sweden

[9]Department of Neurodegenerative Disease, UCL Institute of Neurology, Queen Square, London, UK

[10]UK Dementia Research Institute at UCL, London, UK

[11]Hong Kong Center for Neurodegenerative Diseases, Hong Kong, China

[12]Wisconsin Alzheimer's Disease Research Center, University of Wisconsin School of Medicine and Public Health, University of Wisconsin-Madison, Madison, Wisconsin, USA

[13]Department of Medicine, Vanderbilt University Medical Center, Nashville, Tennessee, USA

Funding information: Vanderbilt Clinical Translational Science Award, Grant/Award Numbers: UL1-TR000445, UL1-TR002243; Vanderbilt Alzheimer's Disease Research Center, Grant/Award Number: P20-AG068082; Richard Eugene Hickman Alzheimer's Disease Research Endowment; Vanderbilt Memory & Alzheimer's Center; Swedish Research Council, Grant/Award Numbers: #2023-00356, #2022-01018, #2019-02397; European Union's Horizon Europe research and innovation programme, Grant/Award Number: 101053962; Swedish State Support for Clinical Research, Grant/Award Number: #ALFGBG-71320; Alzheimer's Drug Discovery Foundation, Grant/Award Number: #201809-2016862; AD Strategic Fund; Alzheimer's Association, Grant/Award Numbers: #ADSF-21-831376-C, #ADSF-21-831381-C, #ADSF-21-831377-C, #ADSF-24-1284328-C; European Partnership on Metrology; NEuroBioStand, Grant/Award Number: #22HLT07; Bluefield Project; Cure Alzheimer's Fund; Olav Thon Foundation; Familjen Rönströms Stiftelse; Stiftelsen för Gamla Tjänarinnor; Hjärnfonden, Grant/Award Number: #FO2022-0270; Marie Skłodowska-Curie, Grant/Award Number: 860197; European Union Joint Programme – Neurodegenerative Disease Research, Grant/Award Number: JPND2021-00694; National Institute for Health and Care Research University College London Hospitals Biomedical Research Centre; UK Dementia Research Institute, Grant/Award Number: UKDRI-1003; National Center for Advancing Translational Sciences, Grant/Award Number: UL1-TR002243; National Institute of General Medical Sciences, Grant/Award Number: T32-GM007347; National Institute on Aging

Correspondence
Angela L. Jefferson, Vanderbilt Memory and Alzheimer's Center, Vanderbilt University Medical Center, 3319 West End Avenue, Nashville, TN 37203, USA.
Email: angela.jefferson@vumc.org

Abstract

INTRODUCTION: Neuroinflammation may have sex-specific effects on white matter injury and impact the development of dementia.

METHODS: Human chitinase-3-like protein-1 (YKL-40) concentrations at baseline were related to white matter hyperintensity (WMH) volume, free water (FW), and FW-corrected fractional anisotropy using linear effects models (for cross-sectional outcomes) and linear mixed-effects models (for longitudinal outcomes), adjusting for demographic and medical risk factors. Models were repeated with a sex-interaction term and then stratified by sex.

RESULTS: In stratified analyses, greater baseline YKL-40 concentrations were associated with increased WMHs in females but not males in the parietal (females $p = 0.04$; males $p = .34$) and temporal lobes (females $p = 0.005$; males = $p = 0.71$) longitudinally. YKL-40 associations with FW and FW-corrected fractional anisotropy were null.

DISCUSSION: Results suggest that neuroinflammation is a sex-specific driver of WMHs (but not FW) in females. Differential sequelae of neuroinflammation may be one reason that females have a greater burden of WMHs.

KEYWORDS
aging, Alzheimer's disease, sex differences, white matter disease

Highlights

- Cerebrospinal fluid YKL-40 is associated with white matter hyperintensities in females but not males cross-sectionally and longitudinally.
- Longitudinally, cerebrospinal fluid YKL-40 is associated with white matter hyperintensities in the parietal and temporal lobes, regions that exhibit early pathological changes in Alzheimer's disease .
- Cerebrospinal fluid YKL-40 is not associated with white matter microstructural measures.

1 | INTRODUCTION

White matter hyperintensities (WMHs) seen on magnetic resonance imaging (MRI) are associated with a lower threshold for clinical expression of Alzheimer's disease (AD) and related dementias (ADRD)[1] and a faster rate of cognitive decline.[1] Changes in white matter microstructural integrity can be detected on diffusion MRI before they can be seen on conventional T2-weighted MRI sequences. WMHs and white matter microstructure provide complementary information for understanding cerebral white matter injury in aging and disease.

WMHs are often presumed to reflect small vessel cerebrovascular disease.[2] However, in autosomal dominant AD—where amyloid and tau accumulate at a younger age with fewer co-occurring pathologies or vascular risk factors—both microstructural damage[3] and WMHs[4] develop before the onset of clinical symptoms, suggesting that white matter disease may be a pathogenic process closely tied to AD. However, the relationship between white matter disease and amyloid and tau pathology remains unclear. Females seem to have more prevalent WMHs,[5] a greater accumulation of WMHs over time,[6] and lower fractional anisotropy (FA),[7] often considered a marker of worse microstructural integrity. Females are also disproportionately affected by AD,[8] and differences in white matter burden may contribute to this disparity. The drivers of white matter damage beyond vascular disease and the reason for these observed sex differences, are poorly understood.

Neuroinflammation is a plausible pathway to consider in the development of both white matter injury and observed sex differences in white matter. There are well-established sex differences in immune function and dysregulation.[9] Females are disproportionately affected by autoimmune diseases, and the menopausal transition in mid-life may make females particularly vulnerable to sequela of inflammation in aging.[10] Although animal models and autopsy studies show immune cells[11,12] and inflammatory biomarkers[13,14] at white matter lesions, clinical research characterizing the association between biomarkers of inflammation and white matter disease is inconclusive.[15] This discrepancy may exist because previous studies have primarily

used peripheral blood markers of inflammation,[16] which may not accurately reflect neuroinflammation,[15] or have conducted cross-sectional analyses,[15,17,18] which cannot characterize change over time.

Human chitinase-3-like protein-1 (YKL-40) is an established marker of inflammation expressed primarily by astrocytes in the brain.[19] YKL-40 expression has been shown to correlate with pro-inflammatory cytokines in animal models, and these cytokines drive YKL-40 upregulation in human and mouse astrocytes in vitro.[20] YKL-40 levels are elevated in diseases characterized by ongoing inflammation, including AD.[19,21] Some studies, but not all,[22] suggest that YKL-40 is associated with worse white matter microstructure[23,24] and WMHs.[18,25] Whether sex differences exist in the association between neuroinflammation and white matter disease is unknown.

In this study, we examine cerebrospinal fluid (CSF) YKL-40 in relation to WMHs and white matter microstructure. To measure microstructure, we use free-water (FW) elimination, which allows for the separation of extracellular FW and intracellular (FW-corrected FA) compartments.[26] These metrics correct for partial volume effects and are more sensitive to abnormal brain aging.[27] In addition, we explore how sex modifies the associations between YKL-40 and white matter. We hypothesize that higher levels of YKL-40 will be associated with greater white matter injury in areas vulnerable to AD pathology, including the temporal lobe for WMHs and white matter tracts shown previously to be affected in AD, focusing on the cingulum,[28,29] fornix,[27,30] inferior fronto-occipital fasciculus (IFOF),[28,31] inferior longitudinal fasciculus (ILF),[28,31] and uncinate fasciculus (UF).[28] Because females are disproportionately affected by AD and immune diseases, we hypothesize that these associations will be stronger in females than in males.

RESEARCH IN CONTEXT

1. **Systematic review**: The authors used PubMed and Google Scholar to review literature that explored the relationship between neuroinflammation and cerebral white matter. Although studies have previously explored the relationship between YKL-40 and white matter, less is known about sex differences in the association between neuroinflammation and white matter disease.
2. **Interpretation**: The association between cerebrospinal fluid YKL-40 and white matter hyperintensities is modified by sex, suggesting that neuroinflammation is a sex-specific driver of white matter hyperintensities in females but not males.
3. **Future direction**: Future work should replicate findings in more diverse cohorts and explore how the association between neuroinflammation and white matter degradation relates to cognitive decline.

2 | METHODS

2.1 | Study cohort

As described previously,[32] the Vanderbilt Memory and Aging Project is a longitudinal study investigating vascular health and brain aging. Participants were recruited from 2012 to 2014 and were required to speak English, be ≥60 years of age, have a reliable study partner, and have adequate auditory and visual skills. Exclusion criteria included a cognitive diagnosis other than cognitively unimpaired (CU), early mild cognitive impairment (eMCI),[33] or MCI [34]; heart failure; history of major psychiatric illness or neurologic disease (e.g., stroke, multiple sclerosis); MRI contraindications; head injury with loss of consciousness >5 min; and serious illness that could affect longitudinal participation. Self-report and medical record review were used to determine exclusion criteria. At study entry, participants completed a comprehensive evaluation including a physical examination, clinical interview, fasting blood draw, medication review, cardiac magnetic resonance (CMR) imaging, echocardiogram, multimodal brain MRI, and optional lumbar puncture.

The current study leveraged data collected at baseline (2012–2014), 18-month (2014–2016, 3-year (2015–2018), 5-year (2017–2019), 7-year (2019–2021), and 9-year (2021–2023) follow-up visits. For this study, participants were excluded for missing covariates, MRI outcomes, or CSF biomarker data (Figure S1). The Vanderbilt University Medical Center Institutional Review Board approved the protocol. Written informed consent was obtained before data collection. Due to participant consent restrictions in data sharing, a subset of data is available to others for purposes of reproducing the results or replicating procedures. These data, analytic methods, and study materials can be obtained by contacting the corresponding author.

2.2 | Brain MRI

Between 2012 and 2017, participants were scanned at the Vanderbilt University Institute of Imaging Science on a 3T Philips Achieva system (Best, The Netherlands) with an 8-channel SENSE receiver head coil. In 2017, the system was upgraded to a 32-channel dStream head coil. Imaging parameters have been outlined previously.[30,32] Briefly, from 2012 through 2021, T_1-weighted (repetition time = 8.9 ms, echo time = 4.6 ms, spatial resolution = $1 \times 1 \times 1$ mm^3), T_2-weighted fluid-attenuated inversion recovery (FLAIR) (repetition time = 1100 ms, echo time = 121 ms, spatial resolution = $0.45 \times 0.45 \times 4$ mm^3), and diffusion tensor imaging (DTI) along 32 diffusion gradient vectors (repetition time/echo time = 10,000/60 ms, *b*-value = 1000 s/mm^2, spatial resolution = $2 \times 2 \times 2$ mm^2) were acquired as part of a larger multimodal protocol. In 2021, T_1-weighted (repetition time = 6.5 ms, echo time = 2.9 ms, spatial resolution = $1 \times 1 \times 1$ mm^3) and DTI (repetition time/echo time = 3055/89 ms; *b*-value: 1000 s/mm^2; number of directions: 32, resolution = $2.3 \times 2.3 \times 2.5$ mm^3) sequences were updated.

T_1 images were post-processed using Multi-Atlas for volumes.[35] FLAIR images were post-processed using the Lesion Segmentation Tool toolbox for statistical parametric mapping (SPM8), excluding the cerebellum and brainstem.[36] Scans were individually reviewed and manually corrected for any mislabeling. Manual corrections were then confirmed by a board-certified neuroradiologist blinded to clinical information (L.T.D.) using the medical image processing, analysis, and visualization application. Intracranial volume was calculated based on participant-specific gray matter, white matter, and CSF using T_1-weighed images with SPM8. FLAIR images were segmented into five regions of interest, including the total brain, frontal lobe, temporal lobe, parietal lobe, and occipital lobe using a Montreal Neurological Institute (MNI)305 lobe atlas.[37]

As described previously for diffusion images,[30,38,39] data were corrected for head motion and eddy currents, and brains were extracted from the skull. Corrected images were inputted into custom MATLAB code to calculate FW and FW-corrected fractional anisotropy (FA_{FWcorr}) maps.[26] The FA_{FWcorr} map was registered to an in-house template by a non-linear warp using the advanced normalization tools package.[40] Normalization accuracy was manually assessed. This non-linear warp was then applied to the FW maps. A set of five white matter tractography templates, including the cingulum, fornix, IFOF, ILF, and UF, were collated from several well-established templates.[30,41–43] Using a region of interest–based approach, FW and FA_{FWcorr} metrics were calculated within all five tracts for all participants.

2.3 | Lumbar puncture and biochemical analyses

An optional fasting lumbar puncture was completed at baseline in a subset of participants.[44] CSF was collected with polypropylene syringes from an intervertebral lumbar space with a Sprotte 25-gauge spinal needle (Teleflex Medical, Wayne, PA, USA). Samples were immediately mixed and centrifuged, and supernatants were aliquoted in 0.5-mL polypropylene tubes and stored at −80°C. Human chitinase-3-like-protein-1 Quantikine ELISA Kit (R&D Systems, Inc, Minneapolis, MN, USA) was used to measure CSF YKL-40 concentration in batch. Samples were analyzed in batch using commercially available enzyme-linked immunosorbent assays (ELISA; Fujirebio, Ghent, Belgium) to determine the levels of Aβ42 (Lumipulse® G β-Amyloid1-42) and Aβ40 (Lumipulse® G β-Amyloid1-40). Laboratory technicians who were board-certified and blinded to clinical information processed data. Coefficients of variation (intra-assay) were <10%.

2.4 | Analytical plan

As described previously,[32] covariates were collected at study entry and selected a priori for their potential to confound analytical models. Covariates included age, sex, education, race/ethnicity, Framingham Stroke Risk Profile (FSRP; excluding points for age), cognitive status, intracranial volume, and apolipoprotein E (*APOE*) ε4 status. *APOE* ε4 status was defined as positive (ε2/ε4, ε3/ε4, ε4/ε4) or negative (ε2/ε2, ε2/ε3, ε3/ε3). Amyloid positivity was defined as an $A\beta_{42/40}$ ratio ≤0.072.

Data were visually checked for normality, and WMHs (cm^3) were log-transformed due to the skewed distribution. Prior to analysis, we applied the *Longitudinal ComBat* method[45] to harmonize our longitudinally acquired DTI metrics. *Longitudinal ComBat* inputs included the features to be harmonized (DTI metrics), specification of batch variables (scanner software and DTI sequence version), and specification of a linear mixed-effects model.

Linear regression models cross-sectionally related CSF YKL-40 to log-transformed WMH volumes (total, frontal, parietal, temporal, and occipital volumes) and white matter tract (cingulum, fornix, IFOF, ILF, UF) FW and FA_{FWcorr}. One outcome was used per model. Linear mixed-effects regression models related baseline CSF YKL-40 levels to longitudinal WMH volumes and white matter tract FW and FA_{FWcorr} using the same covariates plus follow-up time and a *YKL-40* × *follow-up time* interaction term. One region of interest was tested per model. Secondary analyses using identical covariates examined sex interaction effects by assessing *YKL-40* × *sex* in cross-sectional models and *YKL-40* × *follow-up time* × *sex* on longitudinal WMH volumes and FW and FA_{FWcorr} for each white matter tract. Models were then stratified by sex (male, female).

In post hoc analysis, FSRP interaction effects were assessed using *YKL-40* × FSRP in cross-sectional models and *YKL-40* × *follow-up time* × *FSRP* on longitudinal WMH volumes. Models were then stratified by FSRP based on median split. Aβ interaction effects were assessed with a YKL-40 × $A\beta_{42/40}$ ratio in cross-sectional models and YKL-40 × follow-up time × $A\beta_{42/40}$ ratio on longitudinal WMH volumes. Models were then stratified by amyloid status (positive, negative).

To determine if results were due to statistical outliers, sensitivity analyses excluded predictor or outcome values >4 SD from the group mean. Multiple comparison correction was performed per hypothesis using a false discovery rate (FDR) based on Benjamini–Hochberg's procedure.[46] Significance was set a priori at $p < 0.05$. All analyses were conducted using R 4.3.1 (www.r-project.org).

3 | RESULTS

3.1 | Participant characteristics

The sample included 151 participants (72.3 ± 6.4 years at study entry, 32% female, 93% non-Hispanic White, and 33% *APOE* ε4 carriers). Fifty-two percent of participants were CU, and 38% had MCI. The mean follow-up time was 5.9 ± 2.4 years, with a mean of 4.4 visits up to 9 total years of follow-up. Females had fewer years of education (p-value < 0.001), were more likely to be amyloid positive (p-value = 0.004) and smaller intracranial volume (ICV; p-value < 0.001, Table 1). There were no sex differences in other covariates, YKL-40 concentration, or neuroimaging outcomes.

TABLE 1 Participant baseline characteristics.

	Total ($n = 151$)	Males ($n = 102$)	Females ($n = 49$)	p-value
Demographic and health characteristics				
Age, years	72.3 ± 6.4	72.3 ± 5.9	72.2 ± 7.3	0.67
Race/ethnicity, % non-Hispanic White	93	94	90	0.34
Education, years	16.1 ± 2.8	16.6 ± 2.5	15.0 ± 2.9	**<0.001**
Diagnosis, % MCI	38	33	47	0.21
APOE ε4, % carrier	50	34	16	0.93
Amyloid positive, %	46	38	63	**0.004**
FSRP, total[a]	6.1 ± 2.7	5.8 ± 2.5	6.7 ± 3.1	0.12
MoCA, total score	25.7 ± 3.1	25.8 ± 2.8	25.4 ± 3.6	0.66
Mean follow-up time, years	5.9 ± 2.4	6.0 ± 2.3	5.6 ± 2.7	0.3
Antihypertensive medication use, %	46	44	51	0.43
Diabetes, %	26	18	8	0.84
Current cigarette smoking, %	2	2	0	0.32
Prevalent CVD, %	5	3	2	0.71
Atrial fibrillation, %	6	4	2	0.96
Left ventricular hypertrophy, %	5	2	3	0.18
Intracranial volume, cm^3	1409 ± 128	1464 ± 100	1294 ± 98	**<0.001**
CSF YKL-40, pg/mL	179 ± 64	183 ± 67	171 ± 56	0.35
WMH neuroimaging markers				
Baseline white matter lesion volume, cm^3	13.9 ± 19.1	13.8 ± 20.1	14.1 ± 17.1	0.89
Baseline log-transformed white matter lesion volume, cm^3	2.20 ± 0.96	2.20 ± 0.95	2.22 ± 0.99	0.89
Total WMH annual change, mm^3/year	2240 ± 3270	1830 ± 2140	3150 ± 4830	0.16
Temporal WMH annual change, mm^3/year	98 ± 315	60 ± 166	181 ± 501	0.16
Parietal WMH annual change, mm^3/year	628 ± 929	509 ± 657	890 ± 1322	0.13
Frontal WMH annual change, mm^3/year	1230 ± 1720	1060 ± 1250	1620 ± 2430	0.46
Occipital WMH annual change, mm^3/year	286 ± 748	205 ± 551	464 ± 1048	0.15
DTI neuroimaging markers[b]				
Cingulum FW annual change	0.007 ± 0.005	0.007 ± 0.005	0.007 ± 0.007	0.62
Cingulum FA_{FWcorr} annual change	−0.004 ± 0.004	−0.003 ± 0.003	−0.004 ± 0.004	0.86
Fornix FW annual change	0.007 ± 0.006	0.007 ± 0.005	0.007 ± 0.007	0.98
Fornix FA_{FWcorr} annual change	−0.004 ± 0.005	−0.005 ± 0.004	−0.003 ± 0.007	0.98
ILF FW annual change	0.005 ± 0.006	0.005 ± 0.005	0.006 ± 0.006	0.33
ILF FA_{FWcorr} annual change	−0.005 ± 0.004	−0.005 ± 0.004	0.005 ± 0.005	0.98
UF FW annual change	0.006 ± 0.006	0.006 ± 0.006	0.006 ± 0.006	0.32
UF FA_{FWcorr} annual change	−0.003 ± 0.005	−0.004 ± 0.004	−0.002 ± 0.006	0.27
IFOF FW annual change	0.007 ± 0.006	0.008 ± 0.005	0.006 ± 0.007	0.84
IFOF FA_{FWcorr} annual change	−0.005 ± 0.004	−0.005 ± 0.004	−0.005 ± 0.005	0.98

Note: Values denoted as mean ± standard deviation or frequency.
Bold font indicates p-value < 0.05.
Abbreviations: *APOE*, apolipoprotein E; CVD, cardiovascular disease; FSRP, Framingham Stroke Risk Profile; ILF, inferior longitudinal fasciculus; IFOF, inferior fronto-occipital fasciculus; UF, uncinate fasciculus; WMH, white matter hyperintensity; YKL-40, Human chitinase-3-like-protein-1.
[a]A modified FSRP score excluded points assigned to age.
[b]Free-water and free-water corrected fractional anisotropy are unitless measures.

TABLE 2 Baseline YKL-40 concentration associations with WMH volumes.

	β	95% CI	*p*-value	pFDR
Cross-Sectional				
Whole brain	−0.00012	−0.00238, 0.00214	.92	0.95
Temporal lobe	0.00080	−0.00045, 0.00205	.21	0.95
Parietal lobe	−0.00009	−0.00242, 0.00225	.94	0.95
Frontal lobe	−0.00031	−0.00248, 0.00186	.78	0.95
Occipital lobe	0.00005	−0.00152, 0.00162	.95	0.95
Longitudinal				
Whole brain	0.00483	−0.00062, 0.01028	.08	0.14
Temporal lobe	0.00029	−0.00005, 0.00063	.09	0.14
Parietal lobe	0.00171	−0.00007, 0.00349	.06	0.14
Frontal lobe	0.00252	−0.00059, 0.00563	.11	0.14
Occipital lobe	0.00020	−0.00067, 0.00107	.65	0.65

Note: Models were adjusted for age, sex, education, race/ethnicity, *APOE* ε4 status, Framingham Stroke Risk Profile (excluding points assigned for age), cognitive status, and intracranial volume. For cross-sectional analyses, the parameter estimate (*β*) indicates the degree of change in outcomes per 1 unit increase in YKL-40. For longitudinal analyses, the parameter estimate (*β*) is interpreted as the annual changes of outcomes associated with 1 unit change in YKL-40.

Abbreviations: *APOE*, apolipoprotein E; CI confidence interval; pFDR, false discovery rate corrected *p*-value; WMH, white matter hyperintensity; YKL-40, Human chitinase-3-like-protein-1.

3.2 | YKL-40 and white matter hyperintensities

At baseline, there were no cross-sectional associations between CSF YKL-40 concentration and WMH volumes (*p*-values > 0.20, Table 2). YKL-40 interacted with sex on total, parietal, and frontal WMH volumes (*p*-values < 0.05, Figure 1). Higher CSF YKL-40 concentrations were cross-sectionally related to greater total and all lobar WMH volumes in females (*p*-values < 0.04, Table 3) but not males. All cross-sectional associations persisted after the FDR correction and outlier exclusion except for the *YKL-40 × sex interaction* on parietal lobe WMHs, which was modestly attenuated (pFDR-value = .07). In post hoc analysis, YKL-40 interacted with FSRP on temporal, parietal, and occipital WMH volumes (*p*-values < 0.03, Table S1), which persisted after FDR correction (*p*-values = 0.045) and outlier exclusion (*p*-values < 0.02; data not shown). There were no significant associations in stratified models (*p*-values > 0.05; Table S1). YKL-40 did not interact with CSF A*β* (Table S2).

In longitudinal analyses, higher baseline CSF YKL-40 concentrations were not significantly associated with WMH volumes (*p*-values > 0.06; Table 2). YKL-40 interacted with sex on temporal lobe WMH volume only (*p*-value = 0.007; Figure 2), which persisted after FDR correction but not outlier exclusion (data not shown). In stratified analyses, higher CSF YKL-40 concentrations were associated with the progression of whole brain, temporal, and parietal lobe WMHs over time in females only (*p*-values < 0.04, Table 3). The temporal lobe association persisted after FDR correction (pFDR-value = .02) but not outlier exclusion (data not shown). Whole brain and parietal lobe associations were attenuated after FDR correction (pFDR values > .07) but not outlier exclusion (data not shown). In post hoc analysis, YKL-40 did not interact with FSRP (Table S1) or CSF A*β* on WMH volumes longitudinally (Table S2).

3.3 | YKL-40 and white matter microstructure

Cross-sectionally, there was no association between CSF YKL-40 concentration and FW or FA_{FWcorr} metrics (Table 4). YKL-40 interacted with sex on FW in the fornix (*p*-value = 0.01). Higher YKL-40 concentrations were associated with lower fornix FW and FA_{FWcorr} in females (*p*-values < 0.04) but not males (*p*-values > 0.27, Table S3). These associations were attenuated by the multiple comparison corrections (pFDR-values > .22).

Higher baseline CSF YKL-40 concentration was longitudinally associated with increased FA_{FWcorr} in the cingulum (*p*-value = 0.01; Table 4), but this association did not survive FDR correction (pFDR-value = .13). YKL-40 interacted with sex on the cingulum FW metric (*p*-value = 0.04, Table S4), which persisted after outlier exclusion but not FDR correction (pFDR-value = .26). In males, higher baseline YKL-40 concentration was associated with increased FA_{FWcorr} in the cingulum (*p*-value = 0.04), which did not persist with FDR correction (pFDR-value = .15) or outlier exclusion (data not shown). Higher baseline YKL-40 concentration was associated with increased FW in the ILF (*p*-value = 0.01) and UF (*p*-value = 0.04) in males. These effects were attenuated with FDR correction (pFDR-values > .10) but not outlier exclusion (data not shown).

4 | DISCUSSION

This study aimed to better understand the association between neuroinflammation and white matter macrostructure and microstructure and how these associations may differ by sex. We found that among community-dwelling older adults, CSF YKL-40, a marker of neuroinflammation, interacted with sex on the parietal and frontal lobe WMHs cross-sectionally and the temporal lobe WMHs longitudinally. In stratified analyses, greater YKL-40 concentrations were associated with increased WMH volume in females but not males. This female-specific association was observed cross-sectionally in all lobes and related to longitudinal progression of WMHs in the parietal and temporal lobes. YKL-40 associations with FW and FA_{FWcorr} microstructural metrics were null. Our work adds to the field by showing that neuroinflammation relates to the presence and exacerbation of WMHs over time in females but not males.

We expand on previous work that has shown an association between YKL-40 and WMHs[18,25] by characterizing WMH volume by lobe and exploring sex differences in an aging population. Although the etiology of WMHs is not fully understood, our study suggests that neuroinflammation is a sex-specific driver of WMHs in females. Although vascular disease risk, assessed using FSRP, did modify the relationship between YKL-40 and WMHs cross-sectionally, there was

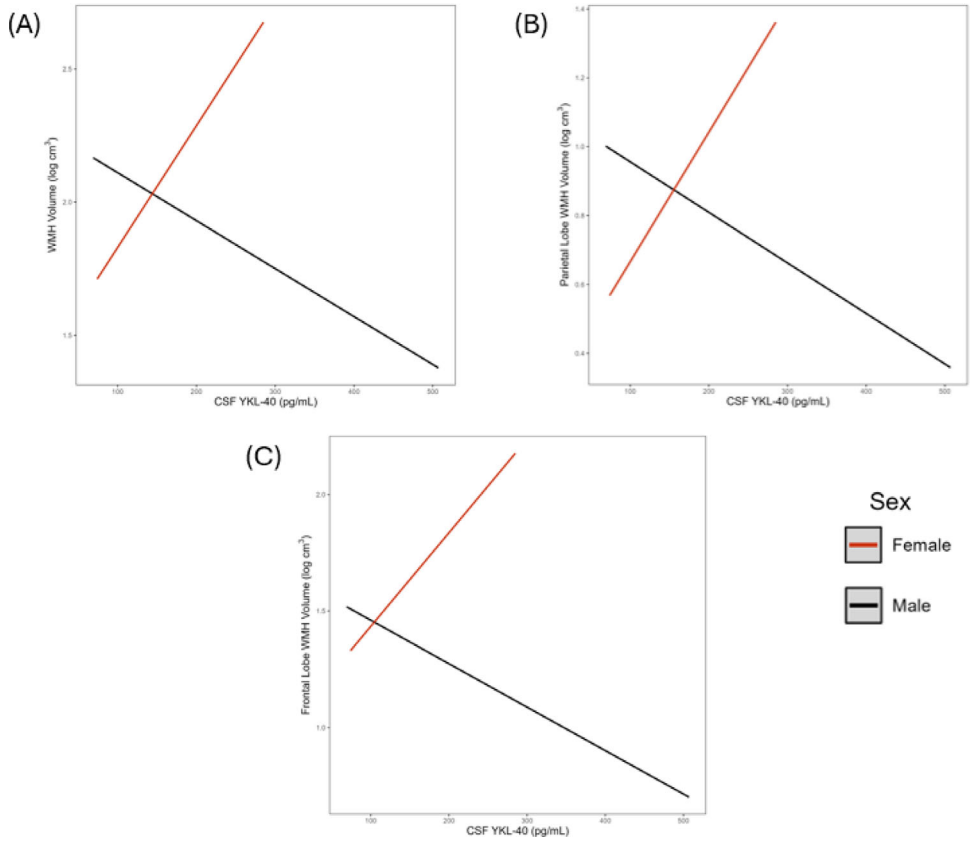

FIGURE 1 YKL-40 × sex interactions on baseline white matter hyperintensity volume. Lines reflect predicted values of white matter hyperintensity volume corresponding to YKL-40 concentration. (A) Total white matter hyperintensity volume. Interaction $p = 0.01$. (B) Parietal lobe white matter hyperintensity volume. Interaction $p = 0.048$. (C) Frontal lobe white matter hyperintensity volume. Interaction $p = 0.02$. CSF, cerebrospinal fluid; WMH, white matter hyperintensity; YKL-40, Human chitinase-3-like-protein-1.

no significant interaction longitudinally, suggesting that cerebrovascular disease may not account for the association between YKL-40 and WMHs that was observed. Although WMHs are often presumed to reflect cerebral small vessel disease,[2] emerging evidence highlights distinct white matter abnormalities in AD.[47] Of interest, longitudinal associations in females were seen in the temporal and parietal lobes, regions that exhibit early pathological changes in AD. Whether neuroinflammation is a cause or consequence of amyloid and tau pathology is debated.[48] We found that amyloid status did not modify the association between YKL-40 and WMHs. However, we were unable to explore whether amyloid positivity modifies the relationship between YKL-40 and WMHs in females due to our sample size. Inflammation may contribute to WMH development independently of amyloid, through mechanisms like endothelial dysfunction, or could interact with amyloid later in the disease as amyloid and tau burden increases. Further work is warranted to determine if the presence of amyloid and tau modifies the association between YKL-40 and temporal and parietal lobe WMHs in females. Several of these associations were attenuated with outlier exclusion, suggesting that this association may not be present when only modest neuroinflammation or WMH burden occurs. It may be that YKL-40 concentrations over a critical value cause an inflammatory cascade resulting in white matter disease onset or progression.[18] Alternatively, the etiology of severe WMH burden may relate to neuroinflammation and differ from the etiology of mild or moderate WMH burden. Some results were attenuated after correction for multiple comparisons; however, females are disproportionately affected by WMHs[5,6] and AD,[8] so our results showing a stronger association between neuroinflammation and white matter hyperintensities in females are biologically plausible.

Our study suggests that the relation between neuroinflammation is different with white matter microstructure versus WMHs. Specifically, sex differences in YKL-40 associations with DTI metrics were modest and did not survive multiple comparison corrections or outlier exclusion. Although evidence suggests that changes in DTI metrics are associated with the subsequent development of WMHs,[49] the etiology underlying white matter microstructure changes may differ from that of WMHs. Additional research is needed to understand the drivers of white matter microstructure change. Although additional work is needed, this study highlights YKL-40's clinical relevance as a possible female-specific biomarker for the risk of WMH development and progression. Alzheimer's disease (or AD) is driven by multiple pathologies, and as such, a combination of therapies will likely be necessary for effective treatment. As new therapies become available, YKL-40 could be integrated into a precision medicine framework, helping to identify women at risk for white matter disease and guide the selection of the most appropriate combination of treatments.

TABLE 3 Baseline YKL-40 × sex interactions on baseline and longitudinal WMH volumes.

	Baseline WMH Volumes				Longitudinal WMH Volumes			
	β	95% CI	*p*-value	pFDR	*β*	95% CI	*p*-value	pFDR
YKL-40 × Sex Interaction								
Whole Brain	0.00637	0.00140, 0.01134	**0.01**	**.04**	0.01156	−0.00003, 0.02314	0.05	.13
Temporal Lobe	0.00260	−0.00018, 0.00537	0.07	.07	0.00117	0.00032, 0.00202	**0.007**	**.04**
Parietal Lobe	0.00522	0.00005, 0.01040	**0.048**	.07	0.00289	−0.00079, 0.00656	0.12	.15
Frontal Lobe	0.00588	0.00110, 0.01066	**0.02**	**.04**	0.00588	−0.00095, 0.01272	0.09	.15
Occipital Lobe	0.00317	−0.00031, 0.00665	0.07	.07	0.00084	−0.00130, 0.00298	0.44	.44
Females								
Whole Brain	0.00556	0.00128, 0.00985	**0.01**	**.03**	0.01705	0.00152, 0.03259	**0.03**	.08
Temporal Lobe	0.00317	0.00073, 0.00561	**0.01**	**.03**	0.00269	0.00085, 0.00454	**0.005**	**.02**
Parietal Lobe	0.00498	0.00064, 0.00931	**0.03**	**.03**	0.00492	0.00010, 0.00973	**0.04**	.08
Frontal Lobe	0.00451	0.00024, 0.00878	**0.04**	**.04**	0.00750	−0.00127, 0.01628	0.09	.12
Occipital Lobe	0.00316	0.00062, 0.00570	**0.02**	**.03**	0.00073	−0.00170, 0.00317	0.55	.55
Males								
Whole Brain	−0.00208	−0.00482, 0.00065	0.13	.31	0.00136	−0.00354, 0.00626	0.59	.85
Temporal Lobe	−0.00020	−0.00173, 0.00133	0.79	.79	0.00006	−0.00027, 0.00040	0.71	.85
Parietal Lobe	−0.00191	−0.00477, 0.00095	0.19	.31	0.00083	−0.00088, 0.00253	0.34	.85
Frontal Lobe	−0.00221	−0.00485, 0.00043	0.10	.31	0.00076	−0.00218, 0.00371	0.61	.85
Occipital Lobe	−0.00068	−0.00265, 0.00129	0.50	.62	0.00010	−0.00089, 0.00109	0.85	.85

Note: Analyses performed on all participants ($n = 151$) and subsequently stratified by sex for females ($n = 49$) and males ($n = 102$). Models were adjusted for age, sex, education, race/ethnicity, *APOE* -ε4 status, Framingham Stroke Risk Profile (excluding points assigned for age), cognitive status, and intracranial volume. For baseline WMH volume, the interaction term was *YKL-40 × sex*. For the sex interaction model, the parameter estimates (*β*) are for the *YKL-40 × sex* interaction term and interpreted as the difference in degree of change in outcomes between male and female participants associated with one unit change in YKL-40. For stratified models by sex, the parameter estimate (*β*) indicates the degree of change in outcomes per one unit increase in YKL-40. For longitudinal WMH volume, the interaction term was *YKL-40 × time × sex*. For the sex interaction model, the parameter estimate (*β*) is for the *YKL-40 × time × sex* interaction term and is interpreted as the difference in annual changes of outcomes between male and female participants associated with a one unit change in YKL-40. For stratified models by sex, the parameter estimate (*β*) is for the *YKL-40 × time* interaction term and is interpreted as the annual change of outcomes associated with one unit change in YKL-40.

Bold font indicates *p*-value < 0.05.

Abbreviations: *APOE*, apolipoprotein E; CI, confidence interval; pFDR, false discovery rate corrected *p*-value; WMH, white matter hyperintensity; YKL-40, Human chitinase-3-like-protein-1.

This study has several strengths, including the longitudinal design over a mean 5.9-year follow-up period in a well-characterized community-based cohort. We used CSF YKL-40, a more local measure of neuroinflammation than plasma biomarkers, which can be of peripheral origin and affected by other systemic diseases. Furthermore, all CSF samples were processed in a core laboratory using quality control procedures. We leveraged high-resolution white matter tractography templates and used FW post-processing, which allowed for the separation of extracellular and intracellular components of the diffusion imaging, thereby reducing partial volume confounding that occurs with conventional diffusion MRI metrics. Nevertheless, this study had several limitations. Participants were predominantly non-Hispanic White, well-educated, and with limited prevalent cardiovascular disease. Although this study population may limit generalizability, the association between neuroinflammation and white matter changes would likely be stronger in a less healthy cohort, which is partly supported by our sensitivity analyses for which findings were attenuated when excluding outliers. White matter tracts in this study were chosen a priori based on vulnerability to AD.[27–29,31,50] Further work is necessary to characterize the relation between YKL-40 and other tracts. In addition, multiple comparisons in our study raise the possibility of false positives. Although this possibility was mitigated with FDR correction, replicating these analyses in a larger, more ethnically, racially, and medically diverse cohort is needed.

The current study demonstrates associations between YKL-40 and WMHs that were present in females but not males. This study adds important insight into why females are disproportionately affected by WMHs and AD and highlights the importance of further exploring the effects of neuroinflammation in neurodegeneration. Future work should replicate findings in more diverse cohorts and explore how the association between neuroinflammation and white matter degradation relates to cognitive decline.

TABLE 4 Association between baseline YKL-40 and DTI measures.

	Free-water				Free-water Corrected FA			
	β	95% CI	*p*-value	pFDR	*β*	95% CI	*p*-value	pFDR
Cross-Sectional								
Cingulum	0.00002	−0.000038, 0.000088	0.44	0.67	0.00000	−0.000047, 0.000040	0.87	0.87
Fornix	−0.00003	−0.000122, 0.000065	0.55	0.67	−0.00004	−0.000094, 0.000015	0.15	0.51
ILF	0.00002	−0.000052, 0.000089	0.60	0.67	0.00001	−0.000035, 0.000064	0.57	0.67
UF	0.00006	−0.000007, 0.000137	0.08	0.45	0.00002	−0.000025, 0.000071	0.35	0.67
IFOF	0.00007	−0.000011, 0.000159	0.09	0.45	−0.00001	−0.000064, 0.000037	0.60	0.67
Longitudinal								
Cingulum	0.00000	−0.000007, 0.000011	0.64	0.71	0.00001	0.000001, 0.000013	**0.01**	0.13
Fornix	0.00000	−0.000004, 0.000015	0.28	0.40	0.00000	−0.000009, 0.000004	0.53	0.67
ILF	0.00001	−0.000001, 0.000018	0.08	0.34	0.00000	−0.000002, 0.000008	0.24	0.40
UF	0.00001	−0.000004, 0.000017	0.21	0.40	0.00000	−0.000001, 0.000010	0.14	0.34
IFOF	0.00000	−0.000009, 0.000012	0.78	0.78	0.00001	−0.000001, 0.000013	0.12	0.34

Note: Models were adjusted for age, sex, education, race/ethnicity, *APOE ε*4 status, Framingham Stroke Risk Profile (excluding points assigned for age), and cognitive status. For cross-sectional analyses the parameter estimates (*β*) indicate the degree of change in outcomes per one unit increase in YKL-40. For longitudinal analyses the parameter estimates (*β*) are for the *YKL-40 × time* interaction term and interpreted as the annual changes of outcomes associated with one unit change in YKL-40.
Bold font indicates *p*-value < 0.05.
Abbreviations: *APOE*, apolipoprotein E; CI, confidence interval; DTI, diffusion tensor imaging; FA, fractional anisotropy; IFOF, inferior fronto-occipital fasciculus; ILF, inferior longitudinal fasciculus; pFDR, false discovery rate corrected *p*-value; UF, uncinate fasciculus; YKL-40, Human chitinase-3-like-protein-1

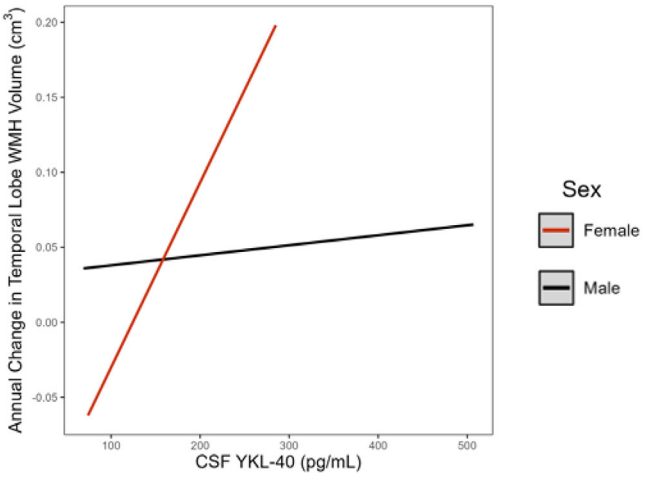

FIGURE 2 YKL-40 × Sex × time interaction on annual change in temporal lobe white matter hyperintensity volume. Lines reflect predicted values of change in temporal lobe white matter hyperintensity volume corresponding to baseline YKL-40 concentration. Interaction $p = 0.007$. CSF, cerebrospinal fluid; WMH, white matter hyperintensity.

ACKNOWLEDGMENTS

The authors would like to thank the dedicated Vanderbilt Memory and Aging Project participants, their loved ones, and our devoted staff and trainees who contributed to the recruitment, screening, enrollment, and follow-up of the cohort. This work was supported by IIRG-08-88733 (A.L.J.), R01-AG034962 (A.L.J.), K24-AG046373 (A.L.J.), R01-AG073439 (L.C.D.), F30-AG085905 (H.A.K.), T32-GM007347 (H.A.K.), UL1-TR000445, and UL1-TR002243 (Vanderbilt Clinical Translational Science Award), P20-AG068082 (Vanderbilt Alzheimer's Disease Research Center), Richard Eugene Hickman Alzheimer's Disease Research Endowment, and the Vanderbilt Memory & Alzheimer's Center. H.Z. is a Wallenberg Scholar and a Distinguished Professor at the Swedish Research Council supported by grants from the Swedish Research Council (#2023-00356, #2022-01018 and #2019-02397), the European Union's Horizon Europe research and innovation programme under grant agreement No 101053962, Swedish State Support for Clinical Research (#ALFGBG-71320), the Alzheimer's Drug Discovery Foundation (ADDF), USA (#201809-2016862), the AD Strategic Fund and the Alzheimer's Association (#ADSF-21-831376-C, #ADSF-21-831381-C, #ADSF-21-831377-C, and #ADSF-24-1284328-C), the European Partnership on Metrology, co-financed from the European Union's Horizon Europe Research and Innovation Programme and by the Participating States (NEuroBioStand, #22HLT07), the Bluefield Project, Cure Alzheimer's Fund, the Olav Thon Foundation, the Erling-Persson Family Foundation, Familjen Rönströms Stiftelse, Stiftelsen för Gamla Tjänarinnor, Hjärnfonden, Sweden (#FO2022-0270), the European Union's Horizon 2020 research and innovation programme under the Marie Skłodowska-Curie grant agreement No 860197 (MIRIADE), the European Union Joint Programme – Neurodegenerative Disease Research (JPND2021-00694), the National Institute for Health and Care Research University College London Hospitals Biomedical Research Centre, and the UK Dementia Research Institute at UCL (UKDRI-1003).

CONFLICT OF INTEREST STATEMENT

T.J.H. serves on the scientific advisory board for *Vivid Genomics* and serves as Deputy Editor for *Alzheimer's and Dementia*: TRCI and senior associate editor for *Alzheimer's and Dementia*. L.T.D. serves as a consultant for Nashville Biosciences, LLC. H.Z. has served at scientific advisory boards and/or as a consultant for Abbvie, Acumen, Alector, Alzinova, ALZpath, Amylyx, Annexon, Apellis, Artery Therapeutics, AZTherapies, Cognito Therapeutics, CogRx, Denali, Eisai, LabCorp, Merry Life, Nervgen, Novo Nordisk, Optoceutics, Passage Bio, Pinteon Therapeutics, Prothena, Red Abbey Labs, reMYND, Roche, Samumed, Siemens Healthineers, Triplet Therapeutics, and Wave, and has given lectures sponsored by Alzecure, BioArctic, Biogen, Cellectricon, Fujirebio, Lilly, Novo Nordisk, Roche, and WebMD. K.B. has served as a consultant, on advisory boards, or on data monitoring committees for Abcam, Axon, Biogen, JOMDD/Shimadzu. Julius Clinical, Lilly, MagQu, Novartis, Roche Diagnostics, and Siemens Healthineers. H.Z. and K.B. are co-founders of Brain Biomarker Solutions in Gothenburg AB, which is a part of the GU Ventures Incubator Program. The remaining authors have no conflicts to disclose. Author disclosures are available in the Supporting Information.

CONSENT STATEMENT

All human subjects provided written informed consent.

ORCID

Amalia J. Peterson https://orcid.org/0000-0002-7015-7957

REFERENCES

1. Debette S, Bombois S, Bruandet A, et al. Subcortical hyperintensities are associated with cognitive decline in patients with mild cognitive impairment. *Stroke*. 2007;38:2924-2930.
2. Alosco ML, Sugarman MA, Besser LM, et al. A clinicopathological investigation of white matter hyperintensities and Alzheimer's disease neuropathology. *J Alzheimers Dis*. 2018;63:1347-1360.
3. Araque Caballero MA, Suarez-Calvet M, Duering M, et al. White matter diffusion alterations precede symptom onset in autosomal dominant Alzheimer's disease. *Brain*. 2018;141:3065-3080.
4. Lee S, Viqar F, Zimmerman ME, et al. White matter hyperintensities are a core feature of Alzheimer's disease: evidence from the dominantly inherited Alzheimer network. *Ann Neurol*. 2016;79:929-939.
5. Than S, Moran C, Beare R, et al. Interactions between age, sex, menopause, and brain structure at midlife: a UK biobank study. *J Clin Endocrinol Metab*. 2021;106:410-420.
6. van den Heuvel DM, Admiraal-Behloul F, ten Dam VH, et al. Different progression rates for deep white matter hyperintensities in elderly men and women. *Neurology*. 2004;63:1699-1701.
7. Peterson A, Sathe A, Zaras D, et al. Sex and APOE ε4 allele differences in longitudinal white matter microstructure in multiple cohorts of aging and Alzheimer's disease. *Alzheimers Dement*. 2025;21(1):e14343. doi:10.1002/alz.14343
8. 2021 Alzheimer's disease facts and figures. *Alzheimers Dement*. 2021;17:327-406.
9. Kivity S, Ehrenfeld M. Can we explain the higher prevalence of autoimmune disease in women? *Expert Rev Clin Immunol*. 2010;6:691-694.
10. Wang Y, Mishra A, Brinton RD. Transitions in metabolic and immune systems from pre-menopause to post-menopause: implications for age-associated neurodegenerative diseases. *F1000Res*. 2020;9.
11. Farkas E, Donka G, de Vos RA, Mihály A, Bari F, Luiten PG. Experimental cerebral hypoperfusion induces white matter injury and microglial activation in the rat brain. *Acta Neuropathol*. 2004;108:57-64.
12. Jalal FY, Yang Y, Thompson JF, Roitbak T, Rosenberg GA. Hypoxia-induced neuroinflammatory white-matter injury reduced by minocycline in SHR/SP. *J Cereb Blood Flow Metab*. 2015;35:1145-1153.
13. Lue LF, Rydel R, Brigham EF, et al. Inflammatory repertoire of Alzheimer's disease and nondemented elderly microglia in vitro. *Glia*. 2001;35:72-79.
14. Rosenberg GA, Sullivan N, Esiri MM. White matter damage is associated with matrix metalloproteinases in vascular dementia. *Stroke*. 2001;32:1162-1168.
15. Low A, Mak E, Rowe JB, Markus HS, O'Brien JT. Inflammation and cerebral small vessel disease: a systematic review. *Ageing Res Rev*. 2019;53:100916.
16. Jefferson AL, Massaro JM, Wolf PA, et al. Inflammatory biomarkers are associated with total brain volume: the Framingham Heart Study. *Neurology*. 2007;68:1032-1038.
17. Poggesi A, Pasi M, Pescini F, Pantoni L, Inzitari D. Circulating biologic markers of endothelial dysfunction in cerebral small vessel disease: a review. *J Cereb Blood Flow Metab*. 2016;36:72-94.
18. Zhang W, Zhou X, Yin J, et al. YKL-40 as a novel biomarker related to white matter damage and cognitive impairment in patients with cerebral small vessel disease. *Brain Res*. 2023;1807:148318.
19. Bonneh-Barkay D, Wang G, Starkey A, Hamilton RL, Wiley CA. In vivo CHI3L1 (YKL-40) expression in astrocytes in acute and chronic neurological diseases. *J Neuroinflammation*. 2010;7:34.
20. Bhardwaj R, Yester JW, Singh SK, et al. RelB/p50 complexes regulate cytokine-induced YKL-40 expression. *J Immunol*. 2015;194:2862-2870.
21. Lananna BV, McKee CA, King MW, et al. Chi3l1/YKL-40 is controlled by the astrocyte circadian clock and regulates neuroinflammation and Alzheimer's disease pathogenesis. *Sci Transl Med*. 2020;12:eaax3519.
22. Melah KE, Lu SY, Hoscheidt SM, et al. Cerebrospinal fluid markers of Alzheimer's disease pathology and microglial activation are associated with altered white matter microstructure in asymptomatic adults at risk for Alzheimer's disease. *J Alzheimers Dis*. 2016;50:873-886.
23. Racine AM, Merluzzi AP, Adluru N, et al. Association of longitudinal white matter degeneration and cerebrospinal fluid biomarkers of neurodegeneration, inflammation and Alzheimer's disease in late-middle-aged adults. *Brain Imaging Behav*. 2019;13:41-52.
24. Hoy AR, Ly M, Carlsson CM, et al. Microstructural white matter alterations in preclinical Alzheimer's disease detected using free water elimination diffusion tensor imaging. *PLoS One*. 2017;12:e0173982.
25. Shi G, Ke D, Gong P, et al. Serum YKL-40 levels and white matter hyperintensities in patients with acute ischemic stroke. *J Inflamm Res*. 2023;16:311-319.
26. Pasternak O, Sochen N, Gur Y, Intrator N, Assaf Y. Free water elimination and mapping from diffusion MRI. *Magn Reson Med*. 2009;62:717-730.
27. Archer DB, Schilling K, Shashikumar N, et al. Leveraging longitudinal diffusion MRI data to quantify differences in white matter microstructural decline in normal and abnormal aging. *Alzheimers Dement*. 2023;15:1-13.
28. Liu Y, Spulber G, Lehtimaki KK, et al. Diffusion tensor imaging and tract-based spatial statistics in Alzheimer's disease and mild cognitive impairment. *Neurobiol Aging*. 2011;32:1558-1571.
29. Adluru N, Destiche DJ, Lu SY, et al. White matter microstructure in late middle-age: Effects of apolipoprotein E4 and parental family history of Alzheimer's disease. *Neuroimage Clin*. 2014;4:730-742.
30. Archer DB, Moore EE, Shashikumar N, et al. Free-water metrics in medial temporal lobe white matter tract projections relate to longitudinal cognitive decline. *Neurobiol Aging*. 2020;94:15-23.

31. Stricker NH, Schweinsburg BC, Delano-Wood L, et al. Decreased white matter integrity in late-myelinating fiber pathways in Alzheimer's disease supports retrogenesis. *Neuroimage*. 2009;45:10-16.
32. Moore EE, Liu D, Bown CW, et al. Lower cardiac output is associated with neurodegeneration among older adults with normal cognition but not mild cognitive impairment. *Brain Imaging Behav*. 2021;15:2040-2050.
33. Aisen PS, Petersen RC, Donohue MC, et al. Clinical core of the Alzheimer's disease neuroimaging initiative: progress and plans. *Alzheimers Dement*. 2010;6:239-246.
34. Albert MS, DeKosky ST, Dickson D, et al. The diagnosis of mild cognitive impairment due to Alzheimer's disease: recommendations from the National Institute on Aging-Alzheimer's Association workgroups on diagnostic guidelines for Alzheimer's disease. *Alzheimers Dement*. 2011;7:270-279.
35. Asman AJ, Landman BA. Non-local statistical label fusion for multi-atlas segmentation. *Med Image Anal*. 2013;17:194-208.
36. Schmidt P, Gaser C, Arsic M, et al. An automated tool for detection of FLAIR-hyperintense white-matter lesions in multiple sclerosis. *Neuroimage*. 2012;59:3774-3783.
37. Toro R, Chupin M, Garnero L, et al. Brain volumes and Val66Met polymorphism of the BDNF gene: local or global effects? *Brain Struct Funct*. 2009;213:501-509.
38. Archer DB, Moore EE, Pamidimukkala U, et al. The relationship between white matter microstructure and self-perceived cognitive decline. *Neuroimage Clin*. 2021;32:102794.
39. Moore EE, Liu D, Pechman KR, et al. Increased left ventricular mass index is associated with compromised white matter microstructure among older adults. *J Am Heart Assoc*. 2018;7:e009041.
40. Avants BB, Epstein CL, Grossman M, Gee JC. Symmetric diffeomorphic image registration with cross-correlation: evaluating automated labeling of elderly and neurodegenerative brain. *Med Image Anal*. 2008;12:26-41.
41. Brown CA, Johnson NF, Anderson-Mooney AJ, et al. Development, validation and application of a new fornix template for studies of aging and preclinical Alzheimer's disease. *Neuroimage Clin*. 2017;13:106-115.
42. Mori S, Oishi K, Jiang H, et al. Stereotaxic white matter atlas based on diffusion tensor imaging in an ICBM template. *Neuroimage*. 2008;40:570-582.
43. Archer D. Tractography Templates for White Matter Microstructure Analysis in Aging and Alzheimer's Disease [Data set]. *Zenodo*. 2024. 10.5281/zenodo.13863955
44. Osborn KE, Liu D, Samuels LR, et al. Cerebrospinal fluid beta-amyloid(42) and neurofilament light relate to white matter hyperintensities. *Neurobiol Aging*. 2018;68:18-25.
45. Beer JC, Tustison NJ, Cook PA, et al. Longitudinal ComBat: a method for harmonizing longitudinal multi-scanner imaging data. *Neuroimage*. 2020;220:117129.
46. Benjamini Y, Hochberg Y. Controlling the False discovery rate: a practical and powerful approach to multiple testing. *J R Stat Soc Ser B Methodol*. 2018;57:289-300.
47. Shirzadi Z, Schultz SA, Yau WW, et al. Etiology of white matter hyperintensities in autosomal dominant and sporadic Alzheimer disease. *JAMA Neurol*. 2023;80:1353-1363.
48. Wyss-Coray T. Inflammation in Alzheimer disease: driving force, bystander or beneficial response? *Nat Med*. 2006;12:1005-1015.
49. Maillard P, Carmichael O, Harvey D, et al. FLAIR and diffusion MRI signals are independent predictors of white matter hyperintensities. *AJNR Am J Neuroradiol*. 2013;34:54-61.
50. Mielke MM, Kozauer NA, Chan KC, et al. Regionally-specific diffusion tensor imaging in mild cognitive impairment and Alzheimer's disease. *Neuroimage*. 2009;46:47-55.

SUPPORTING INFORMATION

Additional supporting information can be found online in the Supporting Information section at the end of this article.

How to cite this article: Peterson AJ, Sun Y, Archer DB, et al. Cerebrospinal fluid YKL-40 relates to white matter hyperintensity progression in females but not males over a 6-year period. *Alzheimer's Dement*. 2025;17:e70110. https://doi.org/10.1002/dad2.70110